INTERFEROMETRIC PHASE STACK DATA FILTER METHOD VIA BAYESIAN CP FACTORIZATION

Rui Wang, Yanan You, Wenli Zhou

School of Information and Communication Engineering, Beijing University of Posts and Telecommunication

IGARSS 2020 - 2020 IEEE International Geoscience and Remote Sensing Symposium | 978-1-7281-6374-1/20/$31.00 ©2020 IEEE | DOI: 10.1109/IGARSS39084.2020.9323383

ABSTRACT

The filter based on tensor decomposition is an effective method to remove the noise of the interferometric phase stack data. The key is to choose the definition of tensor rank and an appropriate tensor decomposition model. The Bayesian CP Factorization (BCPF) -InSAR framework proposed in this paper definites the rank of InSAR tensor by CP rank and decomposes InSAR tensor into low rank tensor, noise tensor and outlier tensor. Compared with several widespread filters, BCPF-InSAR is proved as an effective InSAR tensor filtering method on the simulation data and real data.

Index Terms— synthetic aperture radar (SAR), interferometric SAR (InSAR), tensor decomposition, CP decomposition.

1. INTRODUCTION

Interferometric phase filtering is a significant step in multi-pass synthetic aperture radar interferometry (InSAR) before deformation time-series analysis. Many attempts are devoted to resolving the noise interference in a single interferometric pair. The Goldstein filter [1] is established in frequency domain to improve the performance of reducing noise. The non-local means (NL-means), based on the self-similarity property of images, has been successfully extended to filter an interferometric pair, such as NL-InSAR [2] and NL-SAR [3]. These filters may obtain satisfactory denoising results in most situations, but in the region of phase change rapidly, their performance have a serious deterioration. In addition to the above-mentioned filtering methods for a single interferometric pair, there is a series of filters for multiple interferometric pairs based on tensor decomposition. In fact, the multipass InSAR stack data conforms to the tensor mathematical representation and has low rank structure [4]. Therefore, the tensor-based approach is first applied to phase filtering by Jian et al. [5] as an effective preprocessing step in the framework of ground displacement time-series recovery. More improvements of [5] are proposed in [4] and [6] to further balance the noise removal and the phase information preservation. However, the tensor-based phase filters are established on the assumption that the interferometric phase tensor contains only the low-rank tensor (information) and the noise tensor. Recently, a improved InSAR tensor model is proposed in [7] to decompose the InSAR tensor into low-rank, Gaussain noise and sparse noise tensor.

These filters definite the tensor rank as Tucker rank [4][5][6] or Kronecker based Representation (KBR)[7]. Tucker rank is denoted as $(\text{rank}(\mathbf{X}^{(1)}), \text{rank}(\mathbf{X}^{(2)}), \text{rank}(\mathbf{X}^{(3)}))$ and relaxed as $\sum_i \left\| \mathbf{X}^{(i)} \right\|_*$, where $\mathbf{X}^{(i)}$ is mode-i matricization of tensor $\mathcal{X}$. KBR is a combination of the zero norm of the core tensor acquired by Tucker decomposition and the rank of matricization of the tensor. However, matricization of the tensor destroyed the structure of the tensors and cannot explicitly capture the underlying factors [7].

In order to solve the problem mentioned above, CP rank [8], as a popular tensor rank definition, is analyzed and imported into InSAR phase tensor rank definition. A fully Bayesian probabilistic tensor factorization model with the CP rank based on an improved InSAR phase tensor model is introduced to filter InSAR tensor, named as BCPF-InSAR. The effectiveness of BCPF-InSAR is proved by the experiments on simulation data and real data.

The rest of this paper is organized as follows. Section II describes the limitations of CP-ALS when applied into InSAR tensor. Section III introduces the BCPF-InSAR algorithm in detail. Section IV provides the experiments on simulated and real data. The conclusion is given in the final part.

2. CP DECOMPOSITION OF INSAR TENSOR

The InSAR stack data $\mathcal{T} \in \mathbb{C}^{I_1 \times I_2 \times I_3}$ is a typical third-order tensor as shown in Fig. 2, where the third order denotes the number of interferograms, the first and second order represent an interferogram and the interferogram model is shown as (1).

$$\mathbf{V} = A \cdot e^{j\phi} \tag{1}$$

where A is the amplitude and ϕ is the interferometric phase. Because the focus of this paper is on the phase, the InSAR tensor mentioned later ignores the amplitude and thus the model of the slice in an InSAR tensor is shown as (2).

$$\mathbf{T}_t = \mathcal{T}(:,:,t) = e^{j\phi} \tag{2}$$

Because the phase signal contains a lot of 2π phase jumps, the CP rank should be used to definite the rank of the real and imaginary parts of the InSAR tensor separately.

$$\mathbf{T}_t = \cos\phi + j * \sin\phi = \mathbf{R}_t + j * \mathbf{I}_t \tag{3}$$

where $\mathbf{R}_t$ is the t[th] slice of $\mathcal{R}$ and $\mathcal{R}$ is the real part of $\mathcal{T}$, $\mathbf{I}_t$ is the t[th] slice of $\mathcal{I}$ and $\mathcal{I}$ is the imaginary part of $\mathcal{T}$.

The observed InSAR tensor can be decomposed into low-rank and noise tensor [4][5]. Because the noise is diffused in the real and imaginary part of the InSAR tensor, the mathematical expression of real part of the InSAR tensor decomposition model and its CP rank definition is written as:

$$\mathcal{R} = \mathcal{L}_{\mathcal{R}} + \mathcal{E}_{\mathcal{R}} = \sum_{r=1}^{R_{\mathcal{R}}} (\mathbf{a}_r \circ \mathbf{b}_r \circ \mathbf{c}_r) + \mathcal{E}_{\mathcal{R}} \tag{4}$$

where $\mathcal{L}_{\mathcal{R}}$ is the low rank part of $\mathcal{R}$, $\mathcal{E}_{\mathcal{R}}$ is the noise part of $\mathcal{R}$, $R_{\mathcal{R}}$ is CP rank and $\mathbf{a}_r, \mathbf{b}_r, \mathbf{c}_r$ is the vector acquired by CP decomposition. When given $R_{\mathcal{R}}$, (4) can be solved by (5):

$$\min_{\mathcal{L}} \left\| \mathcal{R} - \mathcal{L}_{\mathcal{R}} \right\|_{\mathrm{F}} = \left\| \mathcal{R} - \sum_{r=1}^{R_{\mathcal{R}}} (\mathbf{a}_r \circ \mathbf{b}_r \circ \mathbf{c}_r) \right\|_{\mathrm{F}} \tag{5}$$

The factor matrix **A**, **B** and **C** are defined as the combination of vectors obtained from CP decomposition, as shown in (6).

$$\begin{aligned} \mathbf{A} &= (\mathbf{a}_1, \mathbf{a}_2, ..., \mathbf{a}_{R_{\mathcal{R}}}) \\ \mathbf{B} &= (\mathbf{b}_1, \mathbf{b}_2, ..., \mathbf{b}_{R_{\mathcal{R}}}) \\ \mathbf{C} &= (\mathbf{c}_1, \mathbf{c}_2, ..., \mathbf{c}_{R_{\mathcal{R}}}) \end{aligned} \tag{6}$$

Eq. (5) can be solved by ALS (Alternating Least Square). With the fixed **B** and **C**, **A** can be calculated by solving (7).

$$\min_{\mathbf{A}} \left\| \mathbf{R}^{(1)} - \mathbf{A}(\mathbf{C} \odot \mathbf{B})^{\mathrm{T}} \right\|_{\mathrm{F}} \tag{7}$$

Therefore, **A** can be updated by (8).

$$\mathbf{A} = \mathbf{R}^{(1)} \left[(\mathbf{B} \odot \mathbf{C})^{\mathrm{T}} \right]^{\dagger} \tag{8}$$

where $[.]^{\dagger}$ is the pseudo-inverse of a matrix.

With **A**, **C** fixed, **B** can be calculated by solving (9).

$$\min_{\mathbf{A}} \left\| \mathbf{R}^{(2)} - \mathbf{B}(\mathbf{C} \odot \mathbf{A})^{\mathrm{T}} \right\|_{\mathrm{F}} \tag{9}$$

Therefore, we can obtain **B** as follows:

$$\mathbf{B} = \mathbf{R}^{(2)} \left[(\mathbf{A} \odot \mathbf{C})^{\mathrm{T}} \right]^{\dagger} \tag{10}$$

With **A**, **B** fixed, **C** can be calculated by solving (11).

$$\min_{\mathbf{A}} \left\| \mathbf{R}^{(3)} - \mathbf{C}(\mathbf{B} \odot \mathbf{A})^{\mathrm{T}} \right\|_{\mathrm{F}} \tag{11}$$

Therefore, we can obtain **C** as follows:

$$\mathbf{C} = \mathbf{R}^{(3)} \left[(\mathbf{A} \odot \mathbf{B})^{\mathrm{T}} \right]^{\dagger} \tag{12}$$

Eq. (8), (10), and (12) are repeated to update the factor matrix **A**, **B** and **C** until they converge.

The filtering effect of the CP decomposition is subject to the CP rank and different InSAR tensors have different appropriate CP ranks. However, the direct calculation of CP rank is a NP-hard problem. Recently, researchers propose the bayesian CP factorization (BCPF), which can automatically determine the CP rank. Therefore, we extend the BCPF to decompose the InSAR tensor with the modifications necessary to adapt the features of the InSAR tensor.

3. BAYESIAN CP FACTORIZATION FOR INSAR TENSOR

The phase noise contains the isolated phase jump-points caused by spatial under-sampling and system thermal noise. Because phase jump-points distribute uniformly and the system thermal noise presents Gaussian distribution, $\mathcal{E}_{\mathcal{R}}$ in (4) should be divide into two parts, i.e. $\mathcal{N}_{\mathcal{R}}$ and $\Omega_{\mathcal{R}}$. Because the noise is diffused in the real part and the imaginary part of the InSAR tensor, the mathematical expression of the model of the real part InSAR phase tensor and its CP rank definition is written as (13).

$$\mathcal{R} = \mathcal{L}_{\mathcal{R}} + \mathcal{N}_{\mathcal{R}} + \Omega_{\mathcal{R}} = \sum_{r=1}^{R_{\mathcal{R}}} (\mathbf{a}_r \circ \mathbf{b}_r \circ \mathbf{c}_r) + \mathcal{N}_{\mathcal{R}} + \Omega_{\mathcal{R}} \tag{13}$$

When given $R_{\mathcal{R}}$, (13) can be solved by (14) to decomposes $\mathcal{R}$ into outlier, noise and low rank tensor.

$$\min_{\mathcal{L}_{\mathcal{R}}} \left\| \Omega_{\mathcal{R}} \odot (\mathcal{R} - \mathcal{L}_{\mathcal{R}}) \right\|_{\mathrm{F}} = \left\| \Omega_{\mathcal{R}} \odot (\mathcal{R} - \sum_{r=1}^{R_{\mathcal{R}}} (\mathbf{a}_r \circ \mathbf{b}_r \circ \mathbf{c}_r)) \right\|_{\mathrm{F}} \tag{14}$$

However, in this framework, it is hard to select appropriate CP rank. Recently, Researchers proposed a Bayesian CP factorization model of incomplete tensors which can automatically determine CP rank, called as BCPF [7]. Based on the position of missing pixels in the InSAR tensor, the rank of the InSAR tensor can be automatically determined and the phase noise can be removed by BCPF, shown as (15).

$$\begin{aligned} (R_{\mathcal{R}}, \mathcal{L}_{\mathcal{R}}) &= \mathrm{BCPF}(\mathcal{R}, \Omega_{\mathcal{R}}) \\ (R_{\mathcal{I}}, \mathcal{L}_{\mathcal{I}}) &= \mathrm{BCPF}(\mathcal{I}, \Omega_{\mathcal{I}}) \end{aligned} \tag{15}$$

where $R_{\mathcal{I}}$ is the CP rank of the imaginary part of the InSAR tensor $\mathcal{I}$, $\mathcal{L}_{\mathcal{I}}$ is the filtered result of $\mathcal{I}$. $\Omega_{\mathcal{R}}$ and $\Omega_{\mathcal{I}}$ are composed of logical values and each pixel in these tensors indicates whether this pixel of $\mathcal{R}$ and $\mathcal{I}$ is outlier, or missed.

Obviously, the phase at the position of jump-points is missed. The position of the outlier in the phase tensor is easy to calculate because the phase at this position is π or $-\pi$. Although the condition is necessary but not sufficient, it provide enough outlier information for BCPF method. Because the real part and the imaginary part of the InSAR tensor cause the outlier in the phase, the outliers are at the

same position of $\mathcal{R},\mathcal{I}$ and the phase tensor. Therefore, $\Omega_{\mathcal{R}}$ and $\Omega_{\mathcal{I}}$ can be calculated by the process mentioned above.

Taking the real part of the InSAR tensor as example, the probabilistic CP decomposition model learned by variational Bayesian framework is shown as (16), called as BCPF method.

$$p(\mathbf{A},\mathbf{B},\mathbf{C},\mathbf{d},\mathcal{N}_{\mathcal{R}}|\mathcal{R}) = \frac{p(\mathbf{A},\mathbf{B},\mathbf{C},\mathbf{d},\mathcal{N}_{\mathcal{R}},\mathcal{R})}{\int p(\mathbf{A},\mathbf{B},\mathbf{C},\mathbf{d},\mathcal{N}_{\mathcal{R}},\mathcal{R})\, d(\mathbf{A},\mathbf{B},\mathbf{C},\mathbf{d},\mathcal{N}_{\mathcal{R}})} \quad (16)$$

where $p(\mathbf{A},\mathbf{B},\mathbf{C},\mathbf{d},\mathcal{E}_{\mathcal{R}},\mathcal{R})$ can be calculated by the probabilistic model shown as (17).

$$p(\alpha,\mathcal{R}) = p(\mathcal{R}|\alpha)p(\mathbf{A}|\mathbf{d})p(\mathbf{B}|\mathbf{d})p(\mathbf{C}|\mathbf{d})p(\mathbf{d})p(\mathcal{N}_{\mathcal{R}}) \quad (17)$$

where α is $(\mathbf{A},\mathbf{B},\mathbf{C},\mathbf{d},\mathcal{N}_{\mathcal{R}})$, $diag(\mathbf{d})$ is the inverse co-variance matrix shared by **A**, **B** and **C**. They are the combinations of vectors obtained from CP decomposition, as shown in (6). And then the detailed computation process of (17) is provided in [7].

However, because of the Eq. (3), $\mathcal{R}$, $\mathcal{I}$ should match the constraint shown as (18), which is ignored when filtering the real and imaginary part of the InSAR phase tensor separately.

$$\mathcal{R}\odot\mathcal{R}+\mathcal{I}\odot\mathcal{I}=\mathcal{O} \quad (18)$$

Therefore, $\mathcal{L}_{\mathcal{R}}$ and $\mathcal{L}_{\mathcal{I}}$ acquired by BCPF method are updated by (19).

$$\mathcal{L}_{\mathcal{R}} = \mathcal{L}_{\mathcal{R}} \odot \frac{\mathcal{O}}{\mathcal{R}\odot\mathcal{R}+\mathcal{I}\odot\mathcal{I}}$$
$$\mathcal{L}_{\mathcal{I}} = \mathcal{L}_{\mathcal{I}} \odot \frac{\mathcal{O}}{\mathcal{R}\odot\mathcal{R}+\mathcal{I}\odot\mathcal{I}} \quad (19)$$

Then, $\mathcal{L}_{\mathcal{R}}$ and $\mathcal{L}_{\mathcal{I}}$ acquired by (19) are updated by BCPF once again. Finally, the filtered phase can be calculated by (20).

$$\text{phase} = \text{angle}(\mathcal{L}_{\mathcal{R}} + j*\mathcal{L}_{\mathcal{I}}) \quad (20)$$

4. EXPERIMENT

In this section, we present and analyze the quantitative and qualitative results to prove the effectiveness of BCPF-InSAR. Experiments are performed on both simulated and real InSAR stack data.

The comparative methods include three traditional filters and two tensor filters: Goldstein filter where the patch is 32×32 and $\alpha = 0.5$, NL-SAR with a 21×21 search window and its patch is set from 3 to 11, NL-InSAR where the search window is 21×21 and the patch is 7×7, HoRPCA and WHoRPCA with fixed parameters as the authors set in the original papers.

The traditional filters denoise the interferograms in the InSAR tensor one by one. The MSE is calculated between the interferogram of the InSAR tensor and its ground truth.The average of MSEs objectively evaluates the filtered tensor acquired by each filter. Furthermore, the means of the number of residues remaining in the filtered interferograms is also used as an effective evaluation.

Two InSAR tensor are simulated with natural terrain and urban terrain. Each tensor has 25 interferograms with 512×512 pixels. 5 dB Guassian noise is implied to the tensor, and 30% pixels in each interferogram are randomly selected to set as π or -π to simulate outliers as shown in Fig. 2.

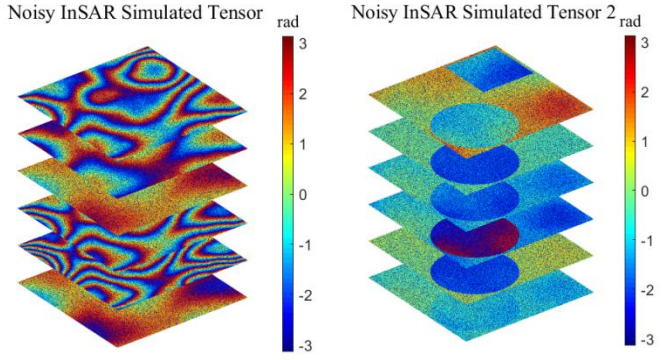

(a) (b)

Fig. 2 Simulated InSAR tensor

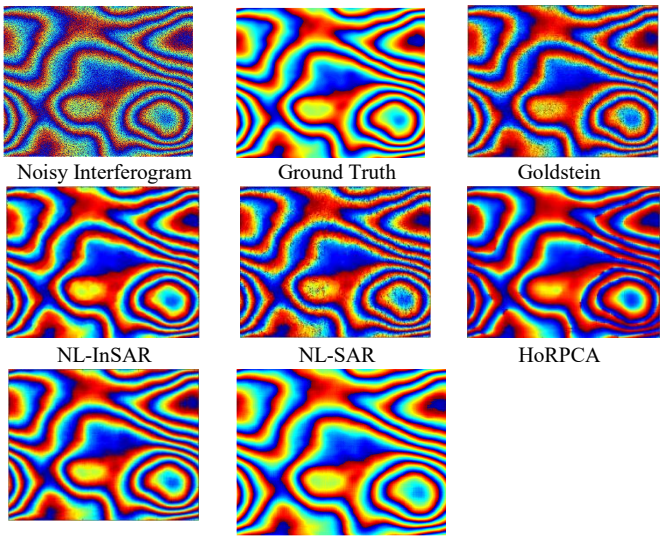

Fig. 3 Filtered Result of the noisy simulated InSAR tensor.

The MSE and remained residues of the comparison filter and BCPF-InSAR are shown in table I. A filtered interferogram in each tensor is selected to evaluate and compare the filters intuitively, as shown in Fig. 3 and Fig. 4. The Goldstein filter and NL-SAR obviously remain some sparse residues, which is clear in visual inspection and confirmed by Table I. NL-InSAR performs well, except in the area where the phase changes rapidly, for example, at the edges of a simulated building. The filtered result of HoRPCA is difficult to preserve the image details because of over smoothing. WHoRPCA improves the problem of excessive smoothing, however, it is still not as good as BCPF-InSAR, which exhibits the satisfied results by preserving the original fringes meanwhile reducing the noise, even in the case of phase jumps. In particular, because BCPF-InSAR inputs the

position of the outliers and recalculate them, the residuals remained in the filtered result is far less than other methods.

Ten SAR complex images acquired by Stentinel-1B from July to November 2018 is selected as experiment data covering Changbai Mountain area in Northeast China. The number of outliers remaining in the filtered interferogram is shown in Table I. A filtered interferogram in the real InSAR tensor is selected to evaluate and compare the filters intuitively, as shown in Fig. 5. The experiment result of real data confirms the conclusions acquired by the simulated data. Compared to other filter methods, BCPF-InSAR exhibit the satisfied performance for suppressing noise and preserving details in real data processing.

TABLE1 MSE on Different Baseline Span

Filter	MSE (tensor1)	Residues (tensor1)	MSE (tensor2)	Residues (tensor2)	Residues (Real Data)
Goldstein	1.73	37488	1.01	62343	96539
NL-SAR	1.48	8820	0.75	8022	53965
NL-InSAR	0.97	25343	0.20	45191	16053
HoRPCA	1.26	7842	0.46	3230	20672
WHoRPCA	0.75	15822	0.46	28490	41943
BCPF-InSAR	0.38	0	0.08	9	0

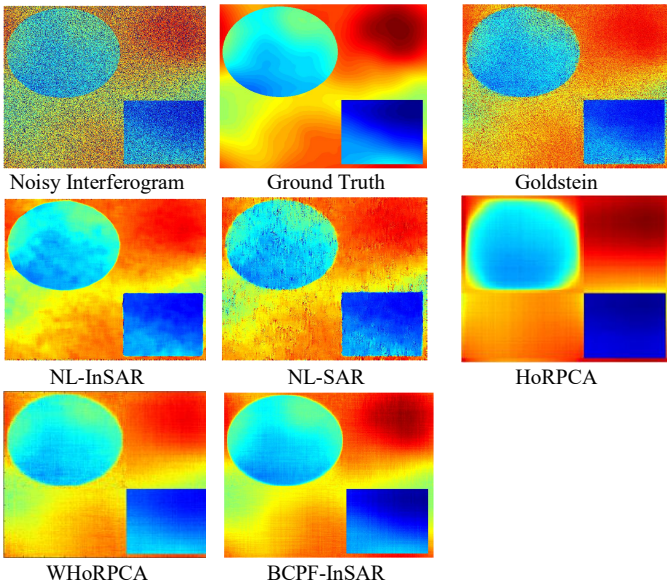

Fig. 4 Filtered Result of the noisy simulated InSAR tensor 2.

5. CONCLUSION

BCPF-InSAR is proposed as a new filter for InSAR stack data, which is established on an effective tensor rank definition, i.e. CP rank. The InSAR stack data is modeled as the combination of low rank tensor, isolated phase jump-points caused by spatial undersampling and system thermal noise. Compared with Tucker rank, CP rank can keep the structural features of the InSAR tensor without using mode-i unfolding of tensor. Moreover, Bayesian CP factorization can automatically determine the appropriate value of CP rank. In phase filtering process, the novel method operates on the real and the imaginary part of the complex InSAR tensor separately with a suitable constraint. Experiments on simulated data and real data prove the effectiveness of the proposed method.

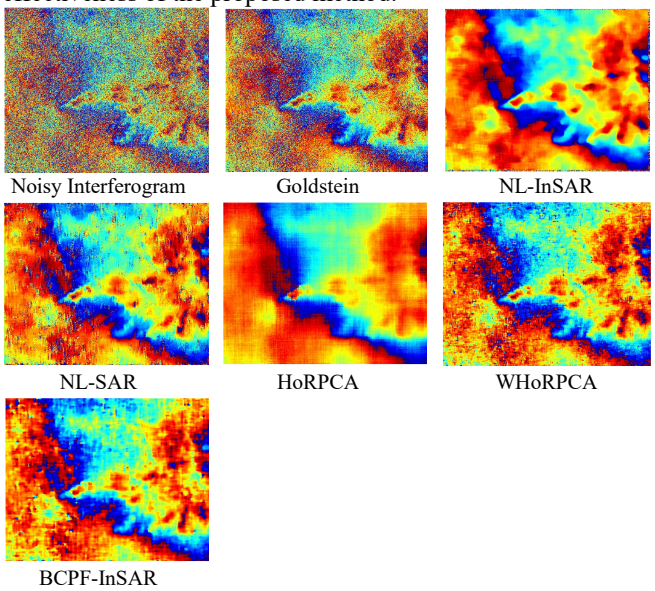

Fig. 5 Filtered Result of the real InSAR tensor.

6. REFERENCES

[1] R. M. Goldstein and C. L. Werner, "Radar interferogram filtering for geophysical applications," *Geophys. Res. Lett.*, vol. 25, no. 21, pp. 4035 – 4038, Nov. 1998.

[2] C.-A. Deledalle, L. Denis, and F. Tupin, " NL-SAR: A unified nonlocal framework for resolution-preserving (Pol)(In)SAR denoising, " *IEEE Trans. Geosci. Remote Sens.*, vol. 53, no. 4, pp. 2021 – 2038, Apr. 2015.

[3] C.-A. Deledalle, L. Denis, and F. Tupin, "NL-InSAR: Nonlocal interferogram estimation," *IEEE Trans. Geosci. Remote Sens.*, vol. 49, no. 4, pp. 1441 – 1452, Apr. 2011.

[4] J. Kang, Y. Wang, M. Schmitt, , and X. X. Zhu, " Object-based multipass insar via robust low-rank tensor decomposition, " *IEEE Trans. Geosci.Remote Sens.*, vol. 56, no. 6, pp. 3062 – 3077, Jun. 2018.

[5] J. Kang, Y. Wang, M. Körner, and X. X. Zhu, "Robust object-based multipass InSAR deformation reconstruction," *IEEE Trans. Geosci. Remote Sens.*, vol. 55, no. 8, pp. 4239 – 4251, Aug. 2017

[6] R. Wang, Y. N. You and W. L. Zhou, "Interferometric Phase stack DEnoiseing via Nonlocal Higher Order Robust PCA Method," *IEEE Access*, vol. 7, pp. 135176 - 135191, Sep. 2019.

[7] Zhao Q, Zhang L, and Cichocki A, "Bayesian CP Factorization of Incomplete Tensors with Automatic Rank Determination," I*EEE Transactions on Pattern Analysis and Machine Intelligence*, vol. 37, no. 9, pp. 1751 - 1763, Sept. 2015.

[8] R. A. Harshman, "Foundations of the PARAFAC procedure: Models and conditions for an "explanatory" multiodal factor analysis," *UCLA Working Papers in Phonetics*, vol. 16, pp. 1–84,1970.